

Cosmic ray composition at high energies: The TRACER project

P.J. Boyle, for the TRACER project¹

Enrico Fermi Institute, University of Chicago, 5640 S Ellis Ave, Chicago, Illinois 60637, USA

Abstract

The TRACER instrument (*Transition Radiation Array for Cosmic Energetic Radiation*) is designed to measure the individual energy spectra of cosmic ray nuclei in long duration balloon flights. The large geometric factor of TRACER (5 m² sr) permits statistically significant measurements at particle energies well beyond 10¹⁴ eV. TRACER identifies individual cosmic ray nuclei with single element resolution, and measures their energy over a wide range, from about 0.5 to 10,000 GeV/amu. This is accomplished with a gas detector system of 1600 single wire proportional tubes and plastic fiber radiators combined with plastic scintillators and acrylic Cerenkov counters. A two week flight in Antarctica in December 2003 has led to a measurement of the nuclear species oxygen to iron up to about 3,000 GeV/amu. As an example, we shall present the energy spectrum and relative abundance for neon and discuss the implication of this result in the context of current models of acceleration and propagation of galactic cosmic rays. The instrument has been refurbished and flown on a second long duration balloon flight in Summer 2006. For this flight, the dynamic range of TRACER has been extended to permit inclusion of the lighter elements B, C and N in the measurement.

Key words:

1. Introduction

Many questions still remain about the origin of cosmic radiation even after nearly 100 years since its discovery. The radiation covers a very large range in energy, 10⁹ to 10²⁰ eV, but exhibits a surprisingly smooth powerlaw energy spectrum, with just a modest break or 'knee' around 10¹⁵ eV. It had been proposed by Baade and Zwicky (1934) that cosmic rays may be generated by supernovae, while Fermi, in his seminal paper in 1949, put forward a mechanism for acceleration due to collisions with magnetized clouds. The Fermi mechanism would produce a power law energy spectrum but could not account for the presence of heavier elements ($Z > 3$) in cosmic rays. In the late 1970s, these basic ideas were reconciled with a model of acceleration in interstellar shock fronts caused by supernova explosions (Bell (1978)). For strong shocks, this model predicts a powerlaw energy spectrum with a slope close to $E^{-2.0}$. However, there appears to be an inherent upper limit to the energies attainable by this mechanism, around $Z \times 10^{14}$ eV (Lagage and Cesarsky (1983)). One might speculate that this limit is reflected in the so called 'knee' in the energy spectrum at 10¹⁵ eV.

Even at 10¹⁵ eV, the gyroradius of cosmic rays in the galaxy is much smaller than the distance to a potential source and so their arrival direction will not reveal the position of their source. To obtain astrophysical information, one measures the absolute intensity and the elemental, and if possible, isotopic composition of cosmic rays as a function of energy. Below the knee, the energy spectra of cosmic ray nuclei are much softer (approximately $\sim E^{-2.7}$) than the expected spectrum from strong shocks. Hence, if the shock acceleration model is correct the propagation of cosmic rays through the galaxy must be dependent on energy.

Indeed, it has been known for a long time (Juliussen et al. (1973)), that the relative abundance of secondary nuclei produced by fragmentation decreases with energy, indicating that the path length of material encountered by cosmic rays propagating through the interstellar medium decreases proportional to $E^{-0.6}$. Detailed analysis of previous composition experiments (Engelmann et al. (1990), Müller et al. (1991)) has inferred a source energy spectrum $\propto E^{-2.2}$ (Swordy et al. (1993)), which is roughly consistent with the shock acceleration model. However, the energy dependence of the cosmic ray pathlength is supported by measurements only up to about 10¹² eV/particle. Hence, detailed measurements at higher energies are needed.

¹ M. Ave, P.J. Boyle, F. Gahbauer, C. Höppner, J. Hörandel, M. Ichimura, D. Müller, A. Romero Wolf

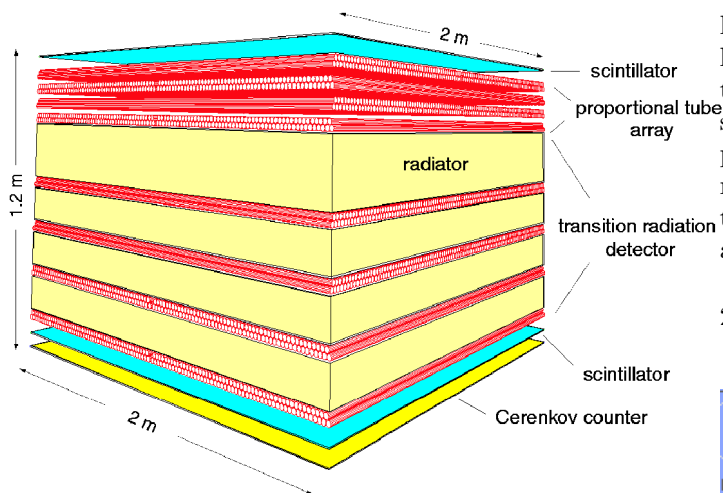


Fig. 1. Schematic drawing of TRACER 2003

2. Description of the TRACER instrument

Direct measurements of the flux of particles at high energy require the availability of an instrument with large exposure factor. This requirement is very difficult to attain with conventional detectors. However, Transition Radiation Detectors (TRDs) may exhibit large area at relatively low weight, and may have good energy response up to particle Lorentz factors of $\gamma \approx 10^5$ (Wakely (2002)). A TRD was first employed in space in the Chicago “Cosmic Ray Nuclei” (CRN) experiment flown aboard the Space Shuttle in 1985 (Swordy et al. (1990)). The results from this experiment (Müller et al. (1991)) still provide the most detailed information on cosmic ray composition at high energies. After the Challenger disaster, continued shuttle flights of CRN were no longer possible, but long duration balloon flights offered a less costly alternative. However, CRN required the use of a heavy pressure gondola to maintain the sensitive multiwire proportional chambers (MWPC) in an environment at atmospheric pressure. This setup is undesirable for balloon flights because the weight of the pressure vessel ($\approx 1,500$ Kg) would represent almost half the allowed science weight of a balloon payload. Therefore we replace the MWPC’s with arrays of single wire proportional tubes (SWPT), which can be operated in external vacuum.

The TRACER experiment is the first balloon borne cosmic ray composition experiment developed using SWPTs to detect transition radiation (Gahbauer et al. (2004)). A design of spiral wound mylar tubes 2cm in diameter, 2m in length and a thickness of about $127 \mu\text{m}$ was chosen (Gahbauer (2003)). Each tube contains a $50 \mu\text{m}$ stainless steel wire stretched through its center. Tubes are arranged into manifolds, consisting of a double layer of 99 tubes, and are filled with a gas mixture containing xenon and methane. The instrument contains 16 manifolds with a total of 1584 tubes (see figure 1). Manifolds are placed in 8 alternative X-Y layers to provide tracking information. Four upper layers (800 tubes) are designed to measure the specific ionization of the incoming cosmic ray particle only, while the four

lower layers are combined with radiators, consisting of blankets of plastic fibers, to produce transition radiation. The total stack of proportional tubes and radiator fibers measures $2\text{m} \times 2\text{m} \times 1.2\text{m}$. Complementing these counters are plastic scintillation counters that act as a trigger and also measure the charge of each particle, and a Cerenkov counter that provides information on the particle’s charge and also an energy measurement in the region of 1-10 GeV/amu.

2.1. Antarctic Balloon Flight

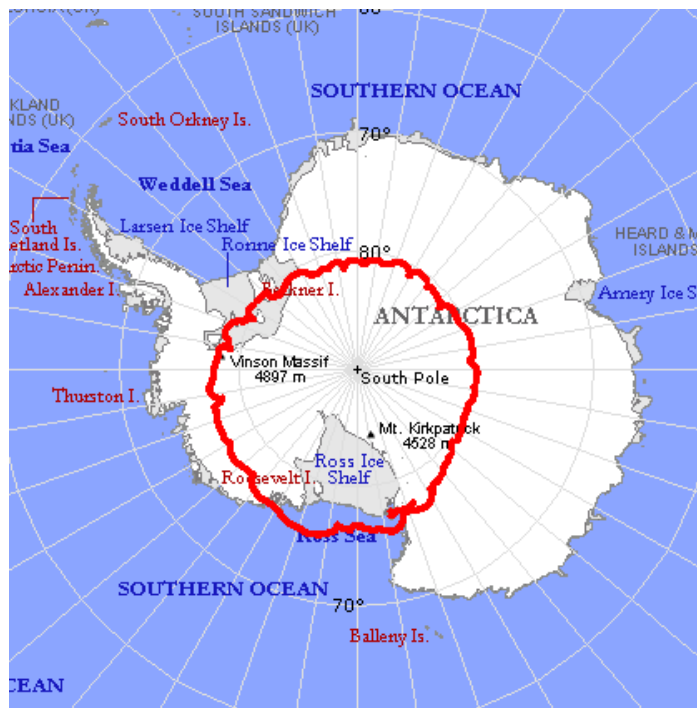


Fig. 2. Trajectory of 2003 TRACER Antarctic Long Duration Balloon Flight.

TRACER was exposed above the atmosphere during a long duration balloon flight of 14 days in Antarctica in December 2003 (Romero-Wolf et al. (2005)). The flight provided a total exposure of 50 m^2 steradian days at an average altitude of 125,000 feet or 3.9 g/cm^2 residual atmosphere. The instrument performed well during the flight. There were no problems with high voltage discharge or corona, and temperature sensors throughout the instrument recorded values in the range $10\text{-}25^\circ\text{C}$, entirely consistent with a thermal analysis carried out before the flight (Cannon and Hörandel (2003)). The quality of the gas in the TRD was monitored during flight and was found to permit stable gas amplification, with variations less than 3%. This performance is much better than that observed on ground, where the gain of the tubes deteriorates with time constants of the order of a day, most likely due to diffusion of oxygen into the tubes. The instrument was fully recovered and returned to Chicago, where a refurbishment for a second long duration balloon flight was subsequently carried out and is described in Section 5.

3. Analysis

3.1. Trajectory Reconstruction

The first step in the analysis of the data is the accurate reconstruction of the cosmic ray trajectories through the instrument. As TRACER has no independent tracking devices we use the entire proportional tube array for this purpose. As a first estimate the path is obtained using the center of each of the tubes hit in an event. This allows an accuracy of 5mm in track position. As a second step, the trajectory is refined by using the fact that the energy deposit in each tube is proportional to the track length in that tube. With this method we achieve an accuracy of 2mm in the lateral track position, corresponding to 3% in total pathlength through all the tubes. The accuracy and efficiency of this method are verified with a GEANT4 simulation of the instrument. Once the trajectory is known, the magnitude dE/dx is determined :

$$\frac{dE}{dx} = \frac{\sum_i dE_i}{\sum_i dx_i} = \frac{\sum \text{energy deposit in tube}(i)}{\sum \text{pathlength in tube}(i)} \quad (1)$$

where the summation goes over all tubes. A cut of $dx_i > 1$ cm is applied to avoid the large fluctuations associated with short pathlengths.

3.2. Charge Analysis

The next stage in the analysis is to determine the charge of each particle using a combination of the plastic scintillation and Cerenkov counters. Trajectory information is used to correct for variations in zenith angle. Spatial variations in the scintillation and Cerenkov counters are corrected using both independent measurements with muons on the ground and cosmic rays collected during the flight. By combining the responses of scintillation and Cerenkov counters we resolve individual charges (see figure 3). Figure 4 shows a charge histogram for all charges obtained from summing along lines of constant charge in figure 3.

3.3. Identification of Low Energy Particles (< 3 GeV/amu)

A balloon flight near the geomagnetic pole exposes the instrument to a large flux of low energy and sub relativistic particles which overwhelms the flux in the TeV region by a factor of 10^4 . These particles must be individually identified and separated with high efficiency from the high energy data set. The separation is achieved by combining the signal from the Cerenkov counter with that of the ionization counter. The energy response for both counters are shown in figure 5. The ionization response, well described by the Bethe-Bloch formula, is represented by the curve labeled dE/dx and the Cerenkov response by the curve labeled CER. Note that the response of the Cerenkov counter must be modified to account for effects by delta rays generated by the primary particle in the instrument. This effect is well

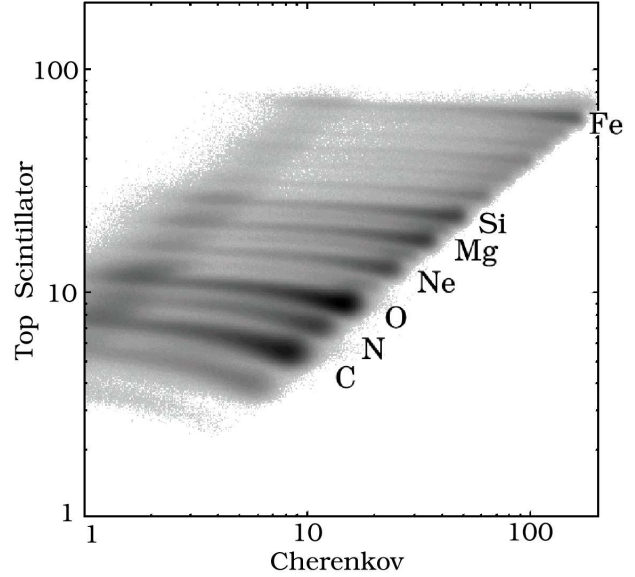


Fig. 3. Scatter plot of top scintillator vs. Cerenkov signal in arbitrary units.

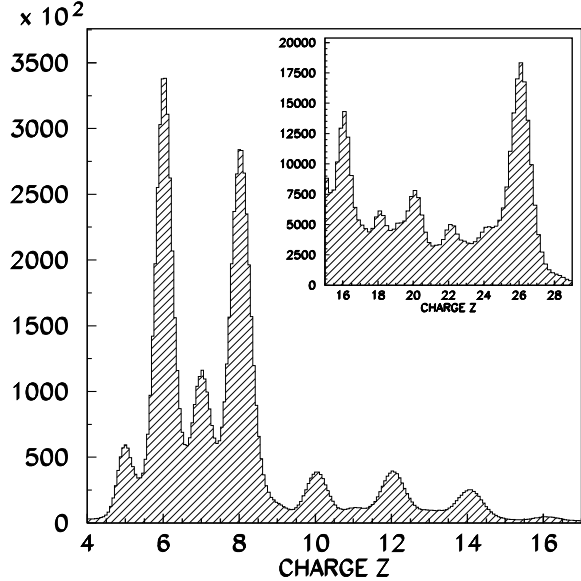


Fig. 4. Charge histogram for all events measured in flight.

understood and has been previously studied and reported (Müller et al. (2003)). The signals from the proportional tube array remain unaffected by delta rays (Romero-Wolf (2005)). Figure 6 illustrates the combined response of the ionization and Cerenkov counters. The black line represents the averaged response obtained from simulations. We see that the Cerenkov signal increases while the ionization signal decreases towards minimum ionization (CER=0.2, Ionization=0.08). At higher energy, the Cerenkov signal saturates and the ionization signal increases due to the relativistic rise in gases. Superimposed in gray are flight data from iron. The data follow closely the pattern predicted by simulations. Although the large flux of low energy particles represents a source of background for the identifica-

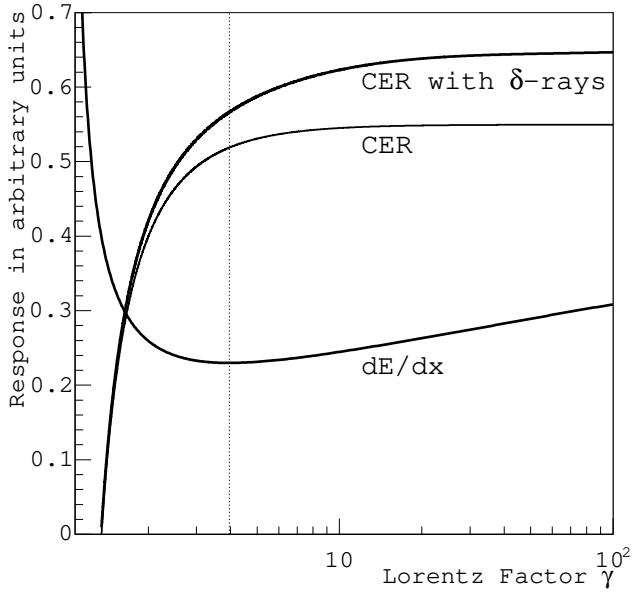


Fig. 5. Energy response of the Cerenkov counter with and without taking into account the δ rays and response function of the specific ionization detector. The dashed line indicates minimum ionization.

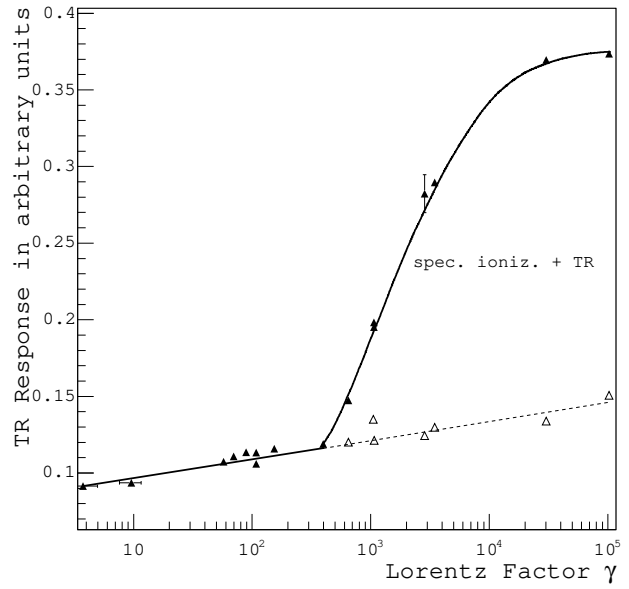


Fig. 7. Energy response of a Transition Radiation Detector used in CRN, as measured at an accelerator L'Heureux and et al. (1990)

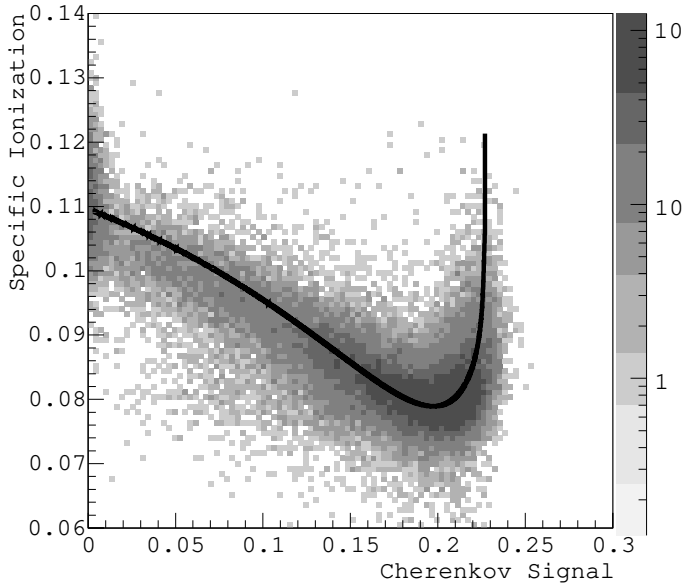


Fig. 6. Scatter plot of dE/dx vs. Cerenkov signals for iron nuclei. The black line is the average response obtained from simulations.

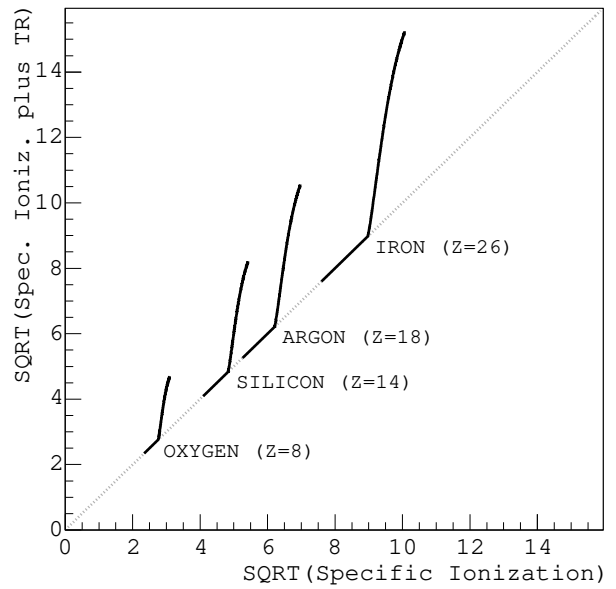


Fig. 8. Correlation of responses of Transition Radiation and specific ionization detectors. Four elements are displayed to illustrate the charge dependence of the responses.

3.4. Identifying the Highest Energy Particles (> 400 GeV/amu)

tion of particles, it also permits to determine exactly the signal levels of minimum ionizing particles at 3 GeV/amu. The Cerenkov signals also are used to determine the energy spectra of each particle species around 1 GeV/amu.

After removing all particles below 3 GeV/amu using the method detailed in section 3.3, the process of identifying the rare high energy particles is achieved through a combination of the measured responses of the ionization counter and the Transition Radiation detector. One of the advantages of using these types of detector is that they can be

calibrated at an accelerator using singly charged particles. Figure 7 shows the measured response for the CRN instrument. Most of the data shown in this figure have been published before (L’Heureux and et al. (1990)). For TRACER, the radiator combination and gas mixtures in the detector are identical to that of CRN, hence the CRN calibration remains valid. The dashed line is the response of the ionization counter, which for TRACER consists of the upper 800 proportional tubes and the solid line represents the TRD, consisting of the lower 800 proportional tubes and radiator combination. At energies between a few GeV/amu and 400 GeV/amu we expect no observable transition radiation. Thus, both signals increase logarithmically with energy, and on average, will lie along the diagonal line in a correlation plot of TRD response vs ionization response (see figure 8). Above 400 GeV/amu, TR becomes observable and the signal from the TRD will increase above the ionization signal. This manifests itself as a deviation from the diagonal in the correlation plot. We expect the signals from individual species to be well separated due to the Z^2 dependence of the signal, with the fluctuations decreasing as $1/Z$ (Swordy et al. (1990), Wakely (2002)).

As an example, figure 9 shows the observed cross correlation between the TRD and the ionization signals for neon nuclei ($Z = 10$) above minimum ionization. The small black points represent the numerous events with energies below the onset of TR. The rare high energy particles with clear TR signals are highlighted. As expected, the data follow the response illustrated in figure 8. Note that the highest energy events (the *TR events*) stand out without any background in other regions of the scatter plot. The most energetic neon nucleus in this sample of data has a total energy of 6×10^{14} eV.

3.5. Derivation of an Absolute Energy Spectrum

We now derive absolute energy spectra over five decades of energy from a few hundred MeV/amu to greater than a TeV/amu. We show here, as an example, the spectrum for neon ($Z = 10$) at the top of the atmosphere. This requires accurate knowledge of exposure factors and efficiencies of the instrument. Table 1 lists the efficiencies due to cuts made on the data which are divided into two data sets : (1) Low Energy (below 3 GeV/amu) and (2) High Energy (above 3 GeV/amu).

The abundance of Low Energy data allows us to make a very strict cut on the zenith angle, thus removing any angle effects in the Cerenkov counter response. Energy bins have been chosen conservatively so that overlap corrections are less than 20%. The center of the energy interval is calculated according to the method of Lafferty and Wyatt (1995). The energy resolution for neon is 15% at 1 GeV/amu, 80% at 100 GeV/amu and 15% at 1000 GeV/amu.

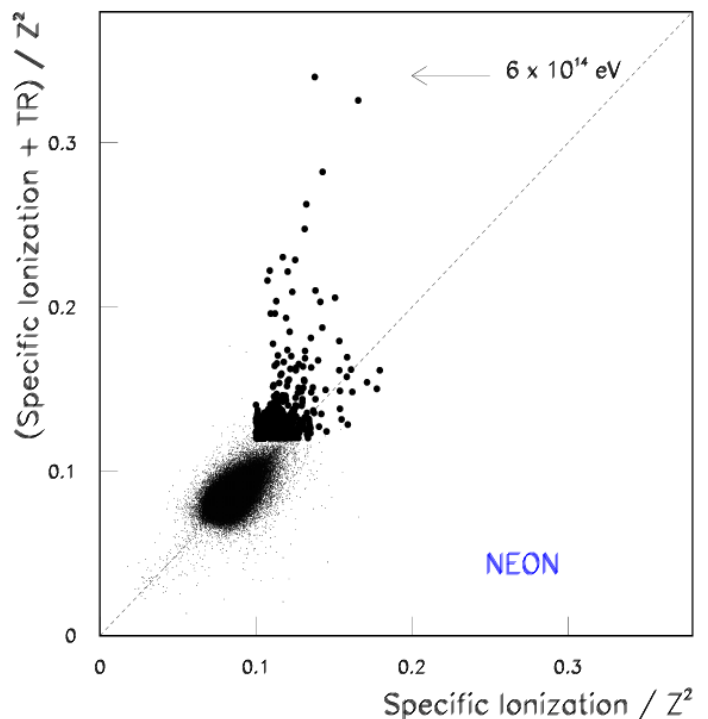


Fig. 9. Scatter plot of TR vs. dE/dx signal for neon nuclei. The highlighted points represent the highest energy events measured with the TRD. As expected the transition radiation events have signals in the dE/dx detector which are well above the minimum ionization level.

Table 1

Exposure and cut efficiencies, i.e. fractions of surviving particles for neon for the 2003 flight.

Cut/Efficiency	Low Energy	High Energy
Zenith Angle	29 - 30°	0 - 60°
Tracking Efficiency	0.95	0.95
Top Scint Efficiency	0.93	0.83
Bot Scint Efficiency	0.95	1.00
Exposure (m² str secs)	76044	1664909

4. Discussion of Results

4.1. Comparison with previous Measurements

The absolute energy spectrum for the single element neon as measured by the TRACER instrument from the 2003 flight is presented as black squares in figure 10. Again, we emphasize that all values are given as absolute intensities with no arbitrary normalizations. We first note the large range in terms of intensity (12 decades) and particle energy (almost 5 decades) covered by TRACER. This has been achieved by combining three complementary measurements in one detector : the Cerenkov counter ($< 10^{11}$ eV), the relativistic rise of the ionization signal in gas ($10^{11} - 10^{13}$ eV) and the TRD ($> 10^{13}$ eV)

TRACER has determined the individual energy spectrum for neon above 10^{14} eV for the first time. The spectrum

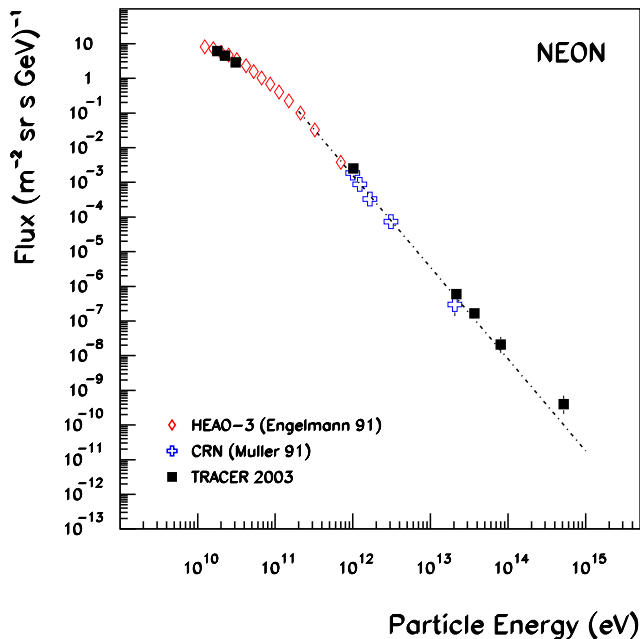


Fig. 10. Differential energy spectrum for neon from TRACER (solid squares), HEAO-3 (open diamonds) and CRN (open crosses). The dashed line represented a power law of $E^{-2.65}$.

does not indicate any steepening towards 10^{15} eV. Below 10^{12} eV we compare our results with measurements from the HEAO-3 satellite and at higher energies with data from CRN on the Space Shuttle. Figure 10 illustrates the good agreement in absolute intensity between the TRACER data and the results from the space borne detectors. The dashed line represents a power law of $E^{-2.65}$ and describes the combined data set above 10^{11} eV. A slight flattening of the spectrum above 10^{14} eV cannot be excluded, and its significance will be discussed in the next section.

4.2. Propagation in the Galaxy

The results from HEAO-3 and CRN have previously been parameterized in a simple propagation model which assumes a dynamic equilibrium between particle production at the source and loss from the Galaxy by diffusive escape or spallation. Good agreement with the measurements has been found if the differential source spectra are proportional to $E^{-2.2}$ and if the escape path length varies as $\Lambda \propto R^{-0.6}$ for rigidities $R > 20$ GV (Swordy et al. (1993)). Figure 11 (solid line) presents the TRACER spectrum for neon as compared to a fit using this model. Note, that for clarity the flux has been multiplied by $E^{2.5}$. The assumption of the model that the escape path length continues as $E^{-0.6}$ up to arbitrary high energies may not be realistic.

A more likely approach may be to introduce an energy independent residual path length Λ_0 in addition to the escape path length, i.e. $\Lambda(E) = AE^{-0.6} + \Lambda_0$. Figure 11 shows three scenarios for different values of the residual path

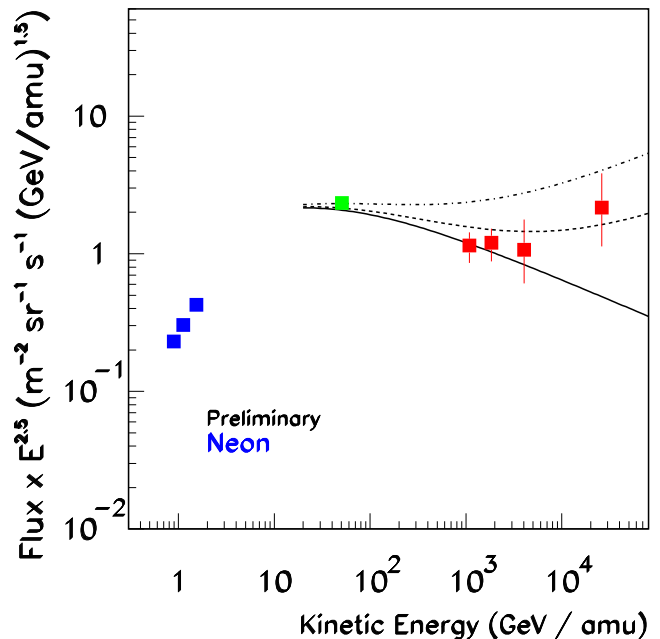


Fig. 11. Differential energy spectrum, multiplied by $E^{2.5}$, for neon as measured by TRACER. The curves refer to a prediction of the simple propagation model from the text. Solid line = $\Lambda_0 = 0$ g/cm², dashed = 0.15 g/cm², dashdot = 0.5 g/cm²

length : $\Lambda_0 = 0$ g/cm² (solid), $\Lambda_0 = 0.15$ g/cm² (dashed), and $\Lambda_0 = 0.5$ g/cm² (dashdot). As can be seen, the value of Λ_0 cannot be much more than 0.15 g/cm² on the basis of this simple analysis. However, determining such a limit with more precision is still work in progress. We are extending the model to the entire data set of the eight individual elements sampled by TRACER and will soon report our conclusions. It would be highly desirable to measure Λ_0 directly by determining the abundance ratio between secondary and primary elements at high energies. An ideal candidate is the boron to carbon ratio. However, the inclusion of these light elements in the measurement was not possible to accomplish in the 2003 flight due to a limited dynamic range in the readout electronics of the TRD.

5. Arctic Flight 2006

We have concluded a second long duration balloon flight of TRACER in 2006, with a refurbished and upgraded instrument launched from Kiruna, Sweden. The instrument was modified to permit a measurement of the secondary to primary ratio, namely the ratio of boron to carbon.

5.1. Upgrades on previous flights

A measurement of the B/C ratio requires high precision in the charge determination. Primary carbon is much more abundant than the secondary boron, and a misidentified carbon nucleus could masquerade itself as boron. To im-

prove the charge resolution over the 2003 flight we doubled the number of PMTs on the bottom scintillation counter, and added a second plastic Cerenkov counter that was placed on top of the instrument. In the 2003 flight, the range of elements probed was limited to $Z=8$ to 26 due to a limited dynamic range of the ASIC AMPLEX chips (Beuville (1990)) used to read out the signals from the proportional tubes. To extend the range to include boron we split the signal resistively for each proportional tube into a Low and High Gain channel, thereby achieving an effective dynamic range of 12 bits or 4096 ADC channels. The doubling of the number of effective proportional tube channels to 3200 required the use of a new DAQ system, the heart of which is a custom Field Programmable Gate Array system.

5.2. Arctic Balloon Flight

TRACER was launched from Kiruna, Sweden at 5am on July 8th 2006. The balloon traveled westward over the Atlantic at an average altitude of 125,000 feet. The initial intent was to let the balloon circumnavigate the North Pole and travel over Russia and land in Sweden or in northern Canada. Unfortunately, Russian overflight permission was not granted for this flight, and hence the flight had to be terminated after four and a half days in northern Canada. The instrument was successfully recovered and the onboard data disks were removed. Figure 12 shows a preliminary charge distribution for a sample of data taken during this flight. The distribution demonstrates that the TRACER instrument is sensitive to charge as low as Helium ($Z=2$). The data analysis is presently underway.

6. Conclusion

The unique feature of the TRACER instrument is the use of gaseous detectors (single wire proportional tubes) to measure both the specific ionization, and specific ionization plus x-ray transition radiation, in order to determine the energy of highly relativistic nuclei (boron to iron). As compared to more conventional techniques, this concept achieves a very favorable ratio of sensitive area to weight; hence, the geometric factor of TRACER by far exceeds that of all other current instruments. The technique also provides a high degree of redundancy because of the multiplicity of measurements taken, and it has the advantage that a complete calibration at accelerators can be and has been performed.

TRACER has been flown in two long duration balloon flights, in 2003 and 2006. The data analysis of the 2003 flight is nearly complete and demonstrates the power of the technique, determining the energy spectra of individual cosmic ray nuclei ($8 \leq Z \leq 26$) over nearly five orders of magnitude in intensity (Boyle et al. (2005)). The small flux of particles at the highest energies is vastly out numbered by cosmic rays of lower energy, but is identified cleanly and without any contamination by low energy background.

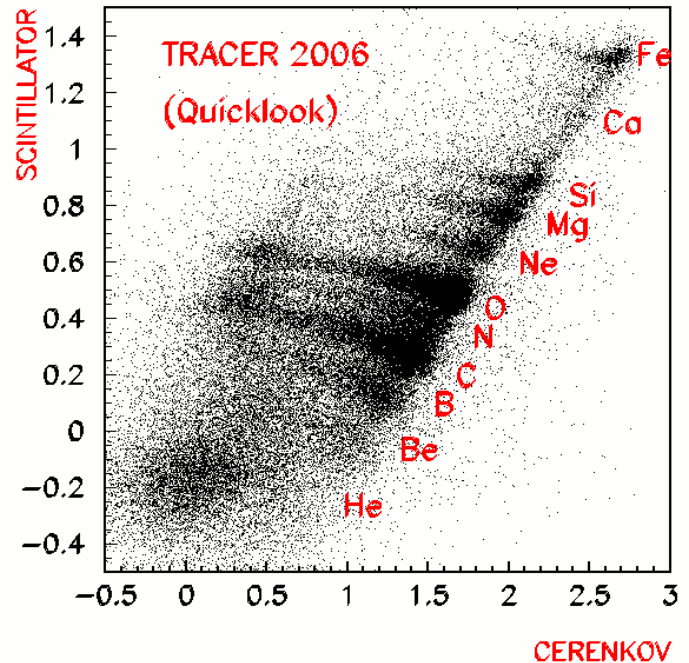


Fig. 12. Charge Distribution from TRACER 2006. These results are from a crude *Quicklook* analysis of 3 hours of data taken during Line of Sight Telemetry. Units are arbitrary.

Therefore, the TRACER results provide a sample of cosmic ray data, that with single charge resolution, extends to the highest energies currently covered in direct measurements, well in excess of 10^{14} eV/particle.

While the results do not reveal any surprising features in the cosmic ray energy spectra at high energies, they begin to provide stringent constraints on the conventional models on galactic propagation. The analysis of the TRACER results in the context of these models is currently still in progress. The second balloon flight of TRACER (2006) will provide very important additional detail, as it will include a measurement of light secondary cosmic ray nuclei, in particular, of the element boron ($Z = 5$).

7. Acknowledgments

This work has been supported by NASA grants NAG5-5305 and NN04WC08G and the Aerospace Illinois Space Grant. We gratefully acknowledge the services of NASA, the Columbia Scientific Balloon Facility, NSF Antarctic Program and ESRANGE.

References

- Baade, W., Zwicky, F., 1934. Cosmic Rays from Supernovae. Proceedings of the National Academy of Science 20, 259–263.

- Bell, A. R., 1978. The Acceleration of Cosmic Rays in Shock Fronts. *Monthly Notices of the Royal Astronomical Society* 182, 147.
- Beuville, E. e., Aug. 1990. AMPLEX, a Low Noise, Low power analog CMOS Signal Processor For Multielement Silicon Particle Detectors. *Nuclear Instruments and Methods A* 288, 157–367.
- Boyle, P. J., Ave, M., Gahbauer, F., Höppner, C., Hörandel, J., Ichimura, M., Müller, D., Romero-Wolf, A., S., W., 2005. Energy Spectra of Heavy Cosmic Ray Nuclei from 0.5 GeV/amu to 10,000 GeV/amu. In: *International Cosmic Ray Conference*. pp. 65–+.
- Cannon, S., Hörandel, J. R., 2003. Thermal Analysis of TRACER, Private Communication.
- Engelmann, J. J., Ferrando, P., Soutoul, A., Goret, P., Juliusson, E., Jul. 1990. Charge composition and energy spectra of cosmic-ray nuclei for elements from Be to Ni - Results from HEAO-3-C2. *Astronomy and Astrophysics* 233, 96–111.
- Gahbauer, F., Hermann, G., Hörandel, J. R., Müller, D., Radu, A. A., May 2004. A New Measurement of the Intensities of the Heavy Primary Cosmic-Ray Nuclei around 1 TeV per amu. *Astrophysics Journal* 607, 333–341.
- Gahbauer, F. H., Jul. 2003. A new measurement of the intensities of heavy cosmic-ray nuclei around 1 TeV/nucleon. Ph.D. Thesis.
- Juliusson, E., Meyer, P., Müller, D., 1973. Cosmic Rays at Very High Energies: Discussion of Some New Results. In: *International Cosmic Ray Conference*. pp. 373–+.
- Lafferty, J. D., Wyatt, T. R., Feb. 1995. Where to stick your data points. The treatment of measurements with wide bins. *Nuclear Instruments and Methods A* 355, 541.
- Lagage, P. O., Cesarsky, C. J., Sep. 1983. The maximum energy of cosmic rays accelerated by supernova shocks. *Astronomy and Astrophysics* 125, 249–257.
- L’Heureux, J., et al., Aug. 1990. *Nuclear Instruments and Methods A* 295, 246.
- Müller, D., Gahbauer, F., Hermann, G., Hörandel, J., Radu, A. A., Jul. 2003. Precise Identification of Heavy Cosmic-Ray Nuclei: The Role of Delta Rays. In: *International Cosmic Ray Conference*. pp. 2245–+.
- Müller, D., Swordy, S. P., Meyer, P., L’Heureux, J., Grunsfeld, J. M., Jun. 1991. Energy spectra and composition of primary cosmic rays. *Astrophysics Journal* 374, 356–365.
- Romero-Wolf, A., Mar. 2005. Energy Loss and Energy Deposit in Single-Wire Proportional Tubes. MSc. Thesis (Unpublished).
- Romero-Wolf, A., Ave, M., Boyle, P. J., Gahbauer, F., Höppner, C., Hörandel, J., Ichimura, M., Müller, D., S., W., 2005. Antarctic Balloon Flight and Data Analysis of TRACER. In: *International Cosmic Ray Conference*. pp. 97–+.
- Swordy, S. P., L’Heureux, J., Meyer, P., Müller, D., Feb. 1993. Elemental abundances in the local cosmic rays at high energies. *Astrophysics Journal* 403, 658–662.
- Swordy, S. P., Müller, D., Meyer, P., L’Heureux, J., Grunsfeld, J. M., Feb. 1990. Relative abundances of secondary and primary cosmic rays at high energies. *Astrophysics Journal* 349, 625–633.
- Wakely, S. P., Aug. 2002. Precision X-ray transition radiation detection. *Astroparticle Physics* 18, 67–87.